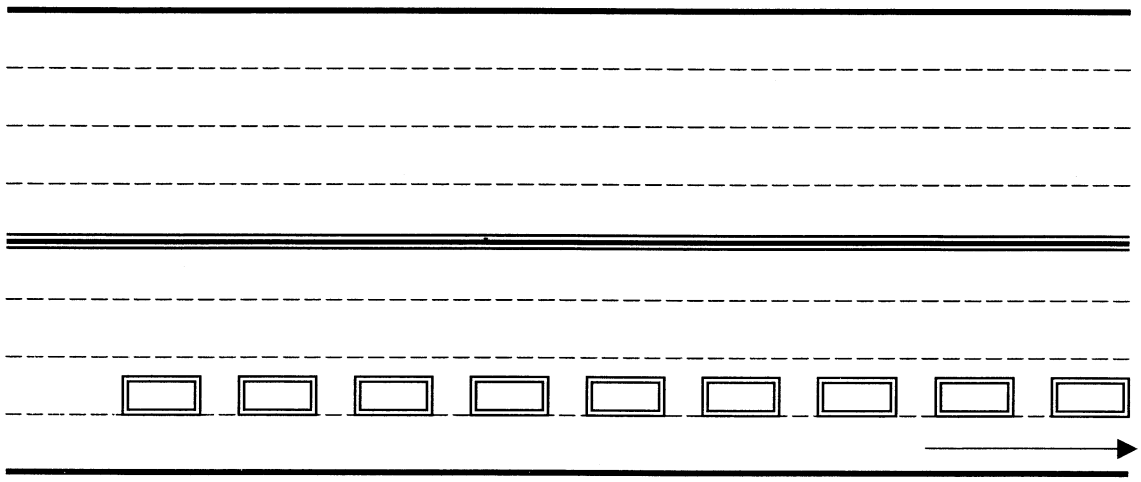

C

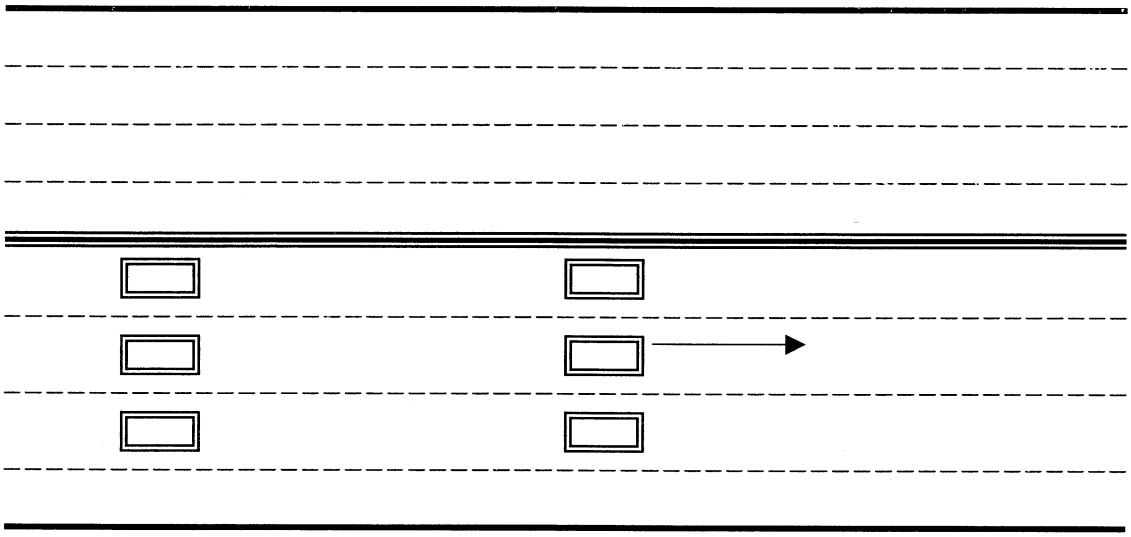

D

Figure 11: Test Set-ups

Open Traffic Tests

Data were also collected during a period of several months on the main and floor trusses to determine typical bridge stress ranges. Both triggered and constant data collection was used. However, triggered data collection was used most to avoid collecting hundreds of megabytes of data that did not show any stress events. This was done for all the gages at panel point 10.

Triggered data collection refers to a method in which the data acquisition system is constantly scanning the gages but does not record anything until strain in a chosen gage exceeds a predetermined limit. The data collection software limited the number of gages one could use as a trigger to three, therefore, one gage on each of the trusses was used as a trigger. In both of the main trusses and in the floor truss, the lower chord was chosen for triggering. This is due to the fact that these chords typically display the highest stress ranges.

The gages on the reversal and the high-tension members were monitored using constant data collection on two separate occasions for about two hours each time. Since these members were such a great distance from the electrical enclosure, taking sample data separately from the gages at panel point 10 proved to be more practical. Therefore a temporary data collection station was set up in a vehicle parked on the walkway below these members. Lead wires were simply dropped to this vehicle during data collection.

Data Collection System

For the truck tests conducted, data were collected using a Campbell Scientific CR9000 data logger. This system is a high-speed multi-channel digital data acquisition system with 16-bit resolution. During these tests, data were collected on between 4 and 18 strain gages at sampling rates of 50 Hz. Running the CR9000 off of its battery gave a cleaner signal than with electrical power. All data were temporarily stored on PCMCIA cards installed on the logger. The data were subsequently copied to a laptop at the end of each test for processing and back-up.

Data were also collected during the long-term monitoring of the bridge using the CR9000 logger. Since the logger was left running for more than a week before the PCMCIA cards were retrieved for data conversion, running off the logger's battery was impossible. Therefore, a temporary power supply running off the bridge's navigational lights was installed and supplied by Mn/DOT. Using external power produced noise in the signal, therefore, to reduce the noise levels in the data a surge protector with a line filter was used.

CHAPTER 5

SUMMARY OF RESULTS

TEST 1 RESULTS

The goal of the first test was to get the greatest response possible under static conditions in the floor truss. Figure 12 shows a time history of the lower chord in the floor truss during this test. There was a discontinuity in the recording before and after the trucks were in position, making it appear as though the load is applied instantly instead of slowly increasing as the trucks neared the gages. The measured strains show that the lower chord goes into tension as expected. The peak stress range is 28 MPa, which is actually the largest stress range recorded in any member in any test.

TEST 2 RESULTS

The goal of the second test was to get the greatest response possible in the main truss. The trucks were driven in the three by three pattern to get a very dense distributed load in all lanes. The measured strains show that the lower chord goes into compression as expected. The greatest stress ranges from this formation of trucks took place in the lower chord and measured 13 MPa. The time history of the response in the lower chord is shown in Figure 13a.

Figures 13b and 13c show the stress ranges in the diagonal and upper chord from the truss during the same event. The stress ranges in the diagonal and upper chord during this test were 10 and 8 MPa, respectively.

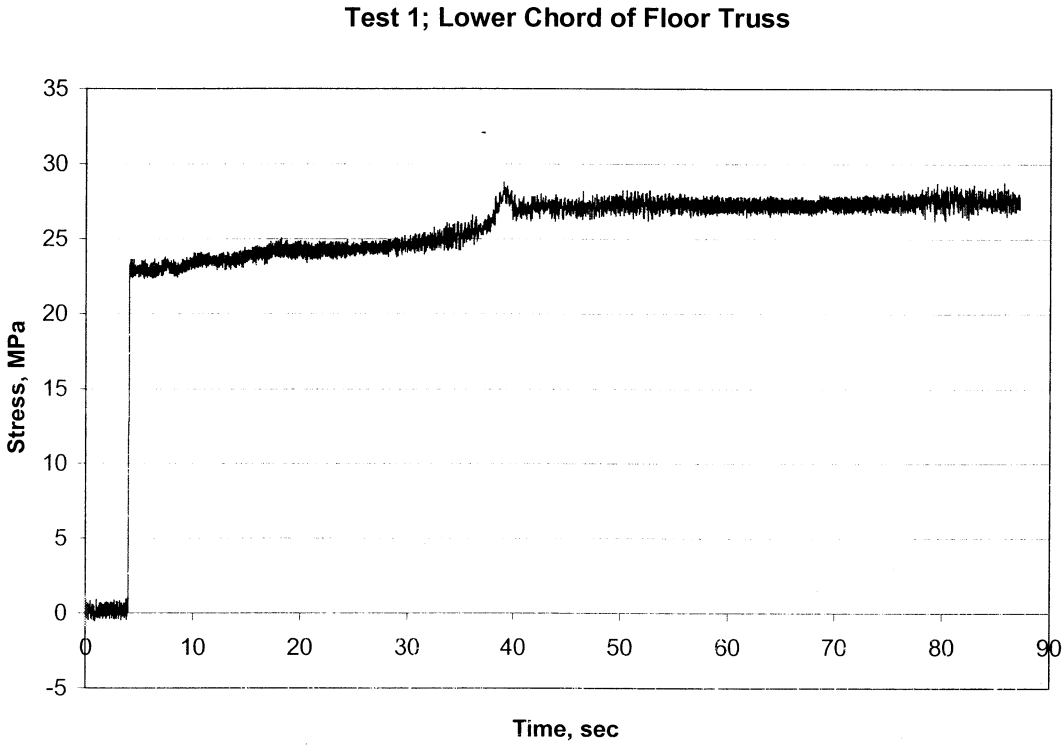

Figure 12: Time History of the Response During Test 1

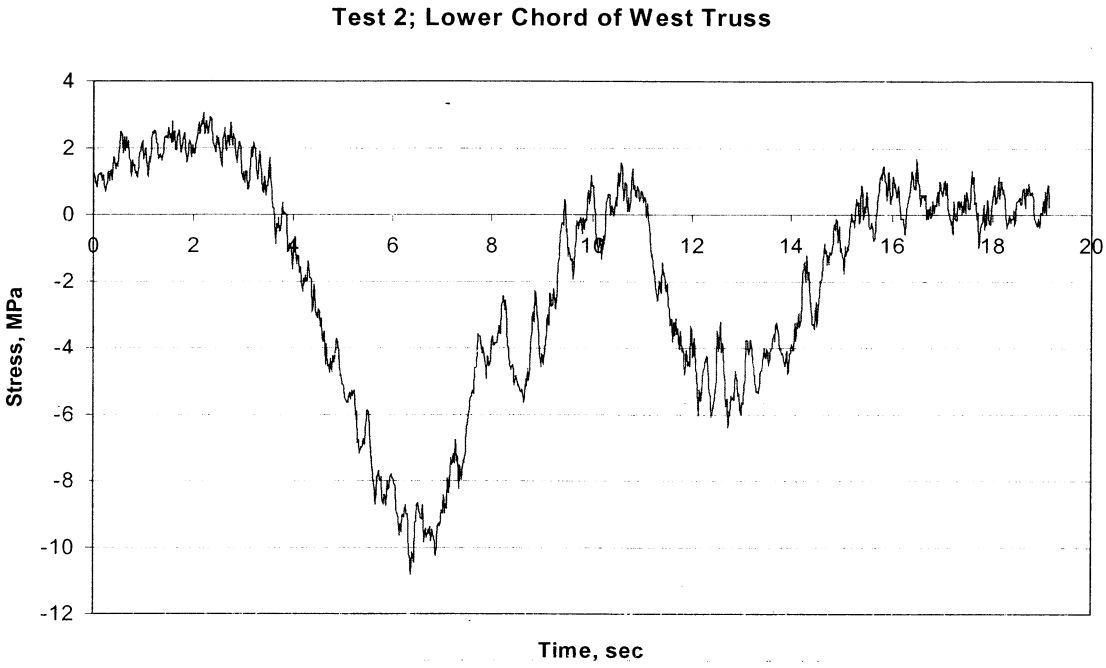
Test 2; Lower Chord of West Truss
Stress, MPa
Time, sec
4
2
0
-2
-4
-6
-8
-10
-12
0
2
6
8
12
14
16
18
20

A

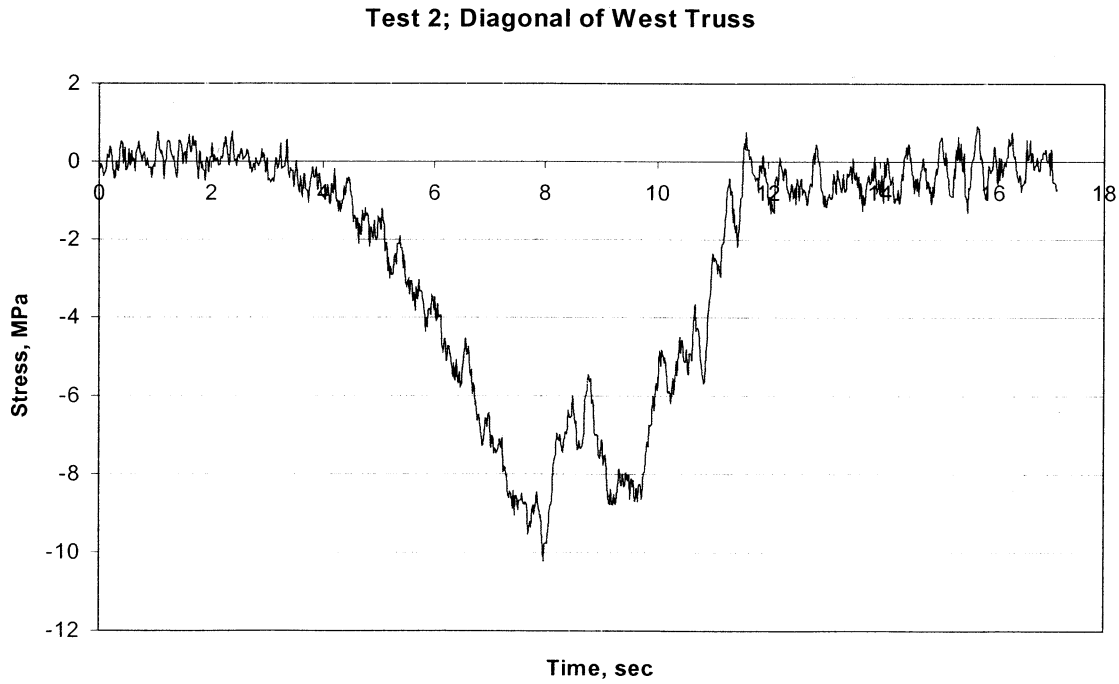
Test 2; Diagonal of West Truss
Stress, MPa
Time, sec
2
0
-2
-4
-6
-8
-10
-12
0
2
6
8
10
18

B

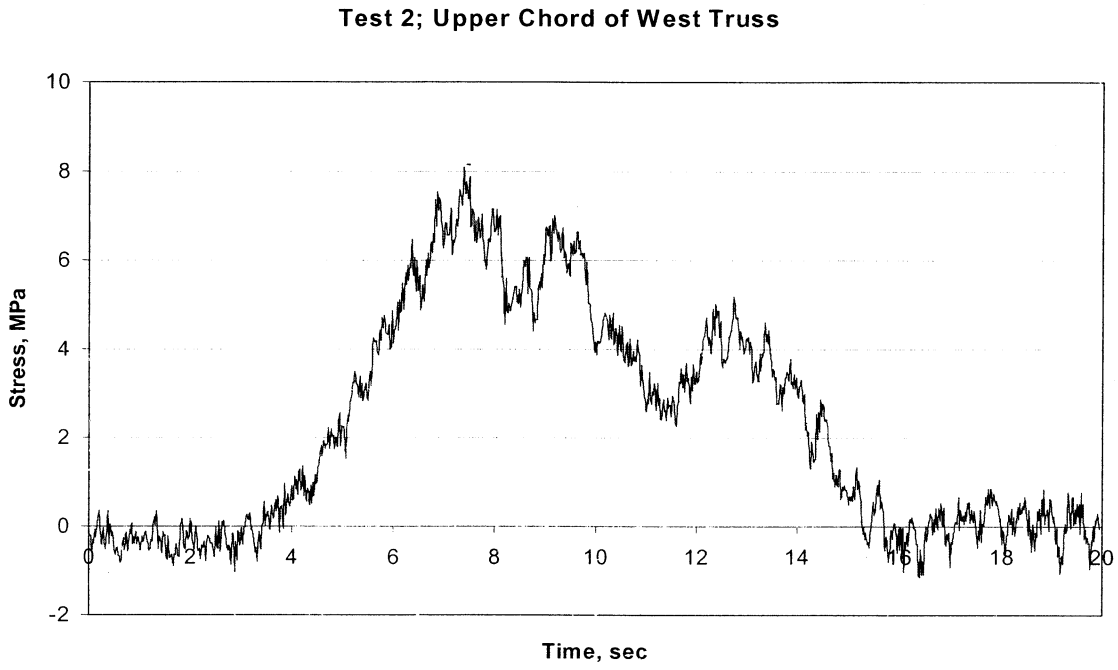

C

Figure 13: Time Histories of the Response During Test 2

TEST 3 RESULTS

The goal of the third test was to load one of the main trusses directly with a line of trucks. However, the trucks were unable to follow any closer than 30.5 meters, resulting in the inability to achieve the desired effect. Instead, the truss responded to the loading of only one truck at a time. The effect of one truck on the truss is barely discernible, and the resulting stress ranges were less than 3.5 MPa. As a result of these low stress ranges, this test will not be discussed further.

TEST 4 RESULTS

This test was another attempt at creating large stress ranges in the floor truss, as well as a means to determine how the load was distributed across the width of the bridge. The maximum stress range for this test occurred in the lower chord of the floor truss and measured 14 MPa. The diagonal and upper chord of the floor truss experienced a maximum stress range of 9 and 7 MPa, respectively. The maximum stress range in the main truss was in the lower chord of the west truss and measured 8 MPa. The maximum stress ranges in the upper chord and diagonal measured 5 and 6 MPa, respectively. The time histories for all gaged members of the floor truss and west truss are shown in Figures 14a-f.

OPEN TRAFFIC RESULTS

Open traffic was monitored during a four-month duration. Continuous data were collected for a limited time and during most of the time data were only recorded when triggered. During this time, the maximum stress ranges in each truss were 13 MPa in the lower chord of the east truss, 12 MPa in the lower chord of the west truss and 26 MPa in the diagonal of the floor truss.

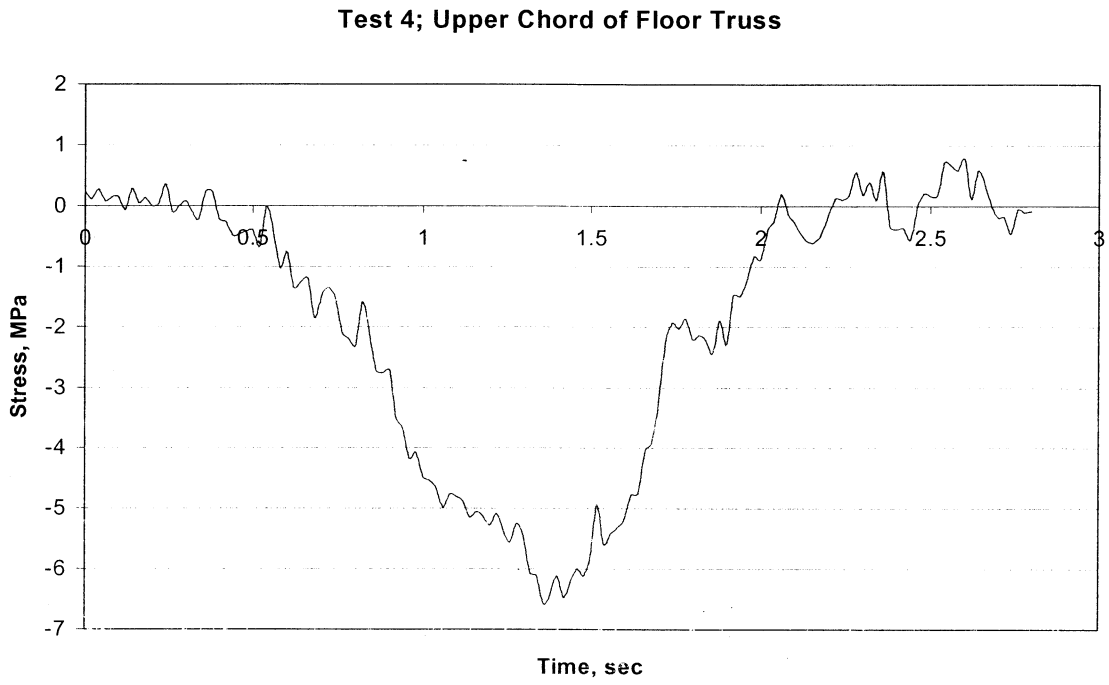
Test 4; Upper Chord of Floor Truss
Stress, MPa
Time, sec
2
1
0
-1
-2
-3
-4
-5
-6
-7
0
0.5
1
1.5
2
2.5
3

A

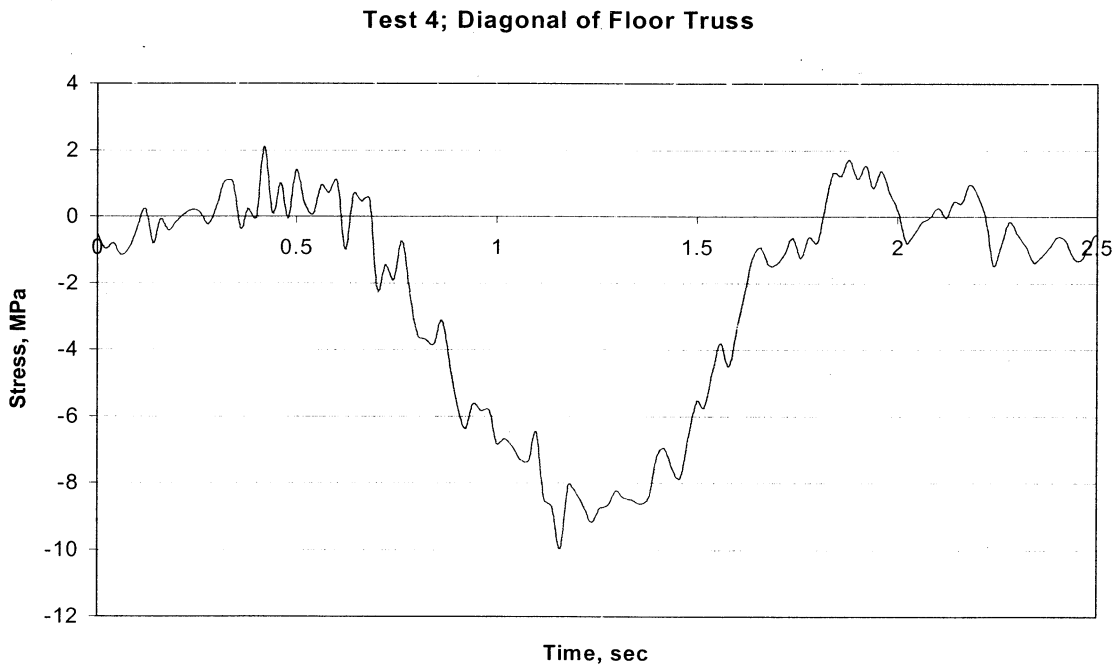
Test 4; Diagonal of Floor Truss
Stress, MPa
Time, sec
4
2
0
-2
-4
-6
-8
-10
-12
0
0.5
1
1.5
2
2.5

B

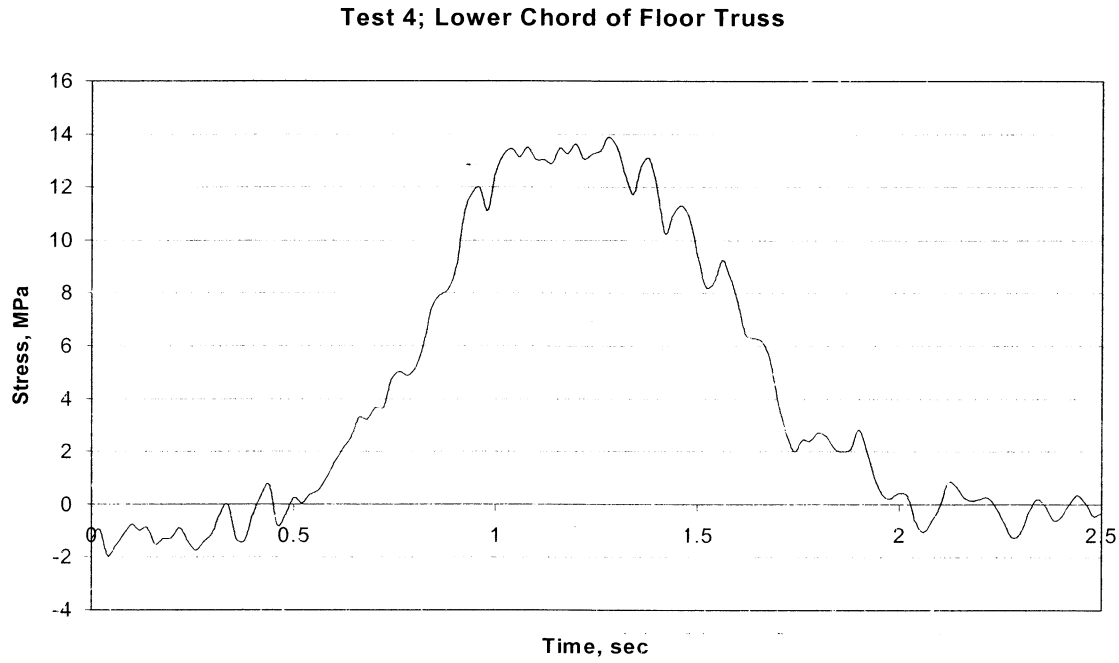
Test 4; Lower Chord of Floor Truss
Stress, MPa
16
14
12
10
8
6
4
2
0
-2
-4
0
0.5
1
1.5
2
2.5
Time, sec

C

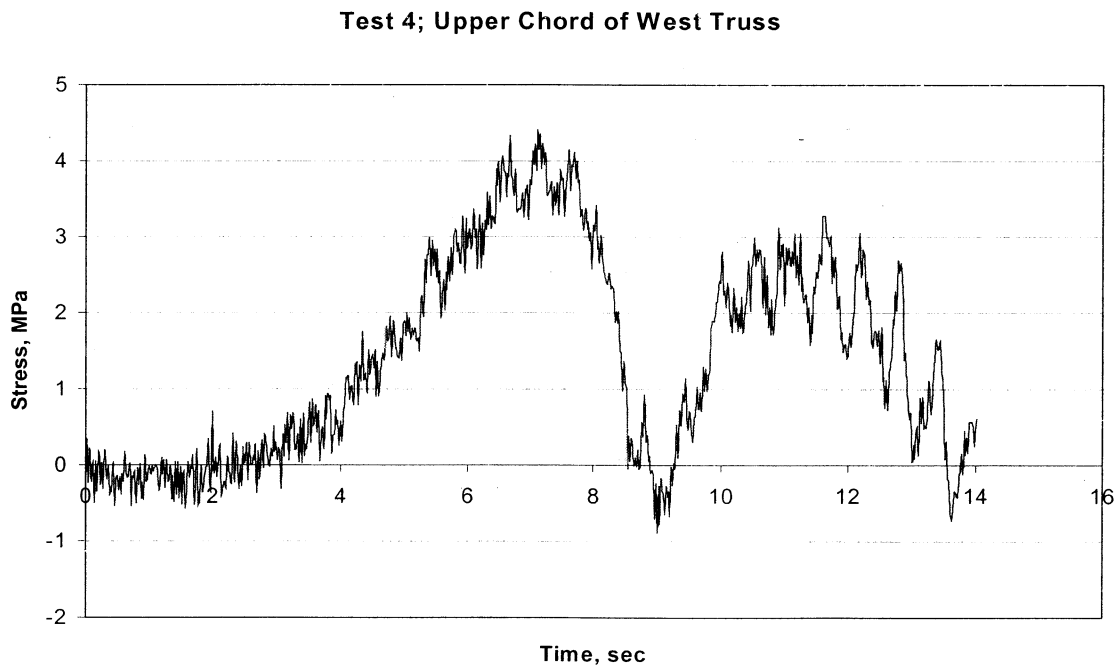
Test 4; Upper Chord of West Truss
Stress, MPa
5
4
3
2
1
0
-1
-2
0
2
4
6
8
10
12
14
16
Time, sec

D

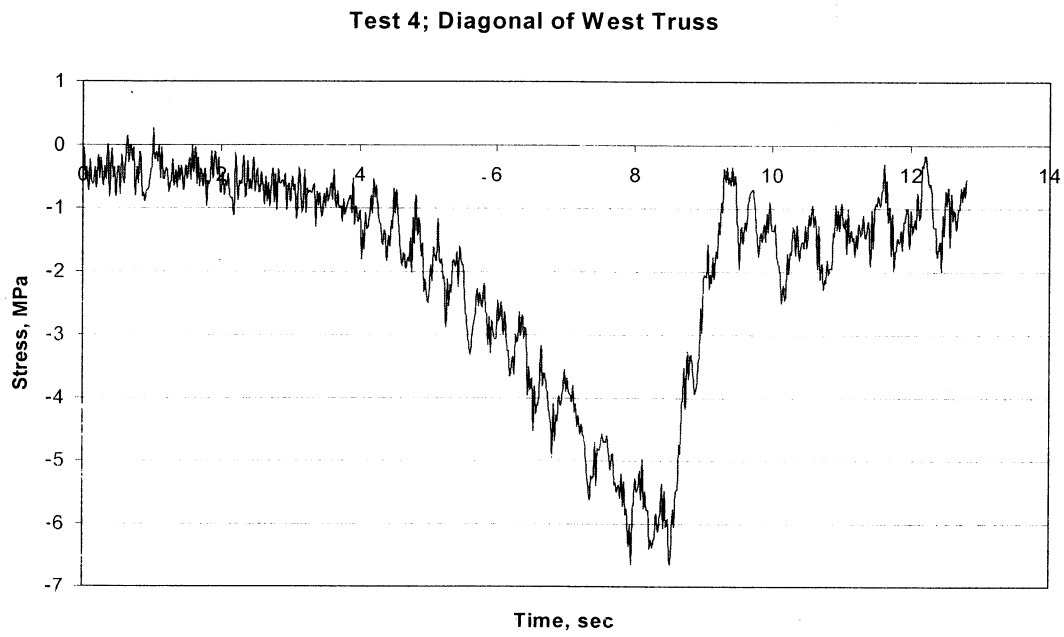

E

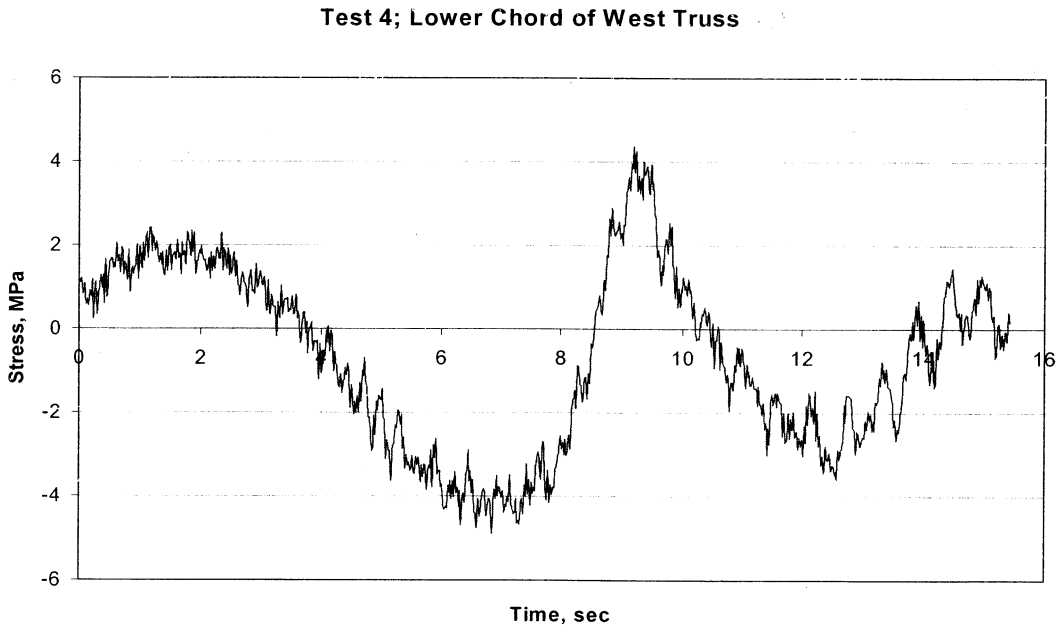

F

Figure 14: Time Histories of the Response During Test 4

Note that these peak stress ranges are comparable to the stress ranges measured during the controlled load tests.

The largest floor truss stress history is presented in Figure 15. The diagonal member is in compression when a load is traveling in the northbound direction, directly over the gaged members, and is in tension when a load is traveling in the southbound direction. Therefore it can be assumed that this large event occurred when two large trucks, each traveling in opposite directions, passed the gaged location within seconds of each other.

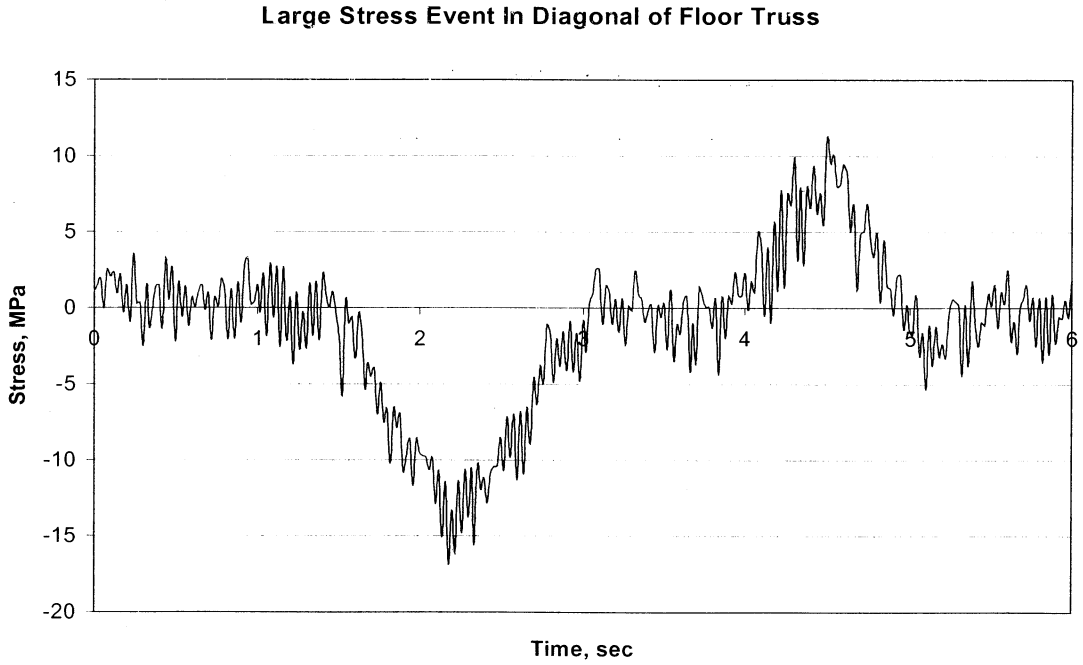

Figure 15: Largest Stress Event Recorded in Open Traffic Conditions

All data collected were imported into an Excel spreadsheet and cycles were counted using an algorithm programmed in Visual Basic in Excel. The algorithm is based on the "level-crossing" cycle counting method. This method counts a new cycle every time the stress crosses from below the mean to above a designated threshold.

To avoid counting thousands of small insignificant fluctuations as stress cycles, cycles were not counted until the stress increased above a threshold stress, which was set at 4.5 MPa, which is less than 15 percent of the smallest fatigue limit (31 MPa for Category E). The stress range associated with a cycle is the algebraic difference between the maximum peak of the stress value between incidents of crossing the cut-off stress and the minimum stress.

This method ignores the fluctuations that occur in a cycle. For example, if one were to apply this method to the main truss, the cycle in Figure 13b would be counted as one cycle with a range of 10 MPa. Note that after the peak, the stress declined to about 5.5 MPa and then increased again to about 8.75 MPa. This intermediate stress range of 3.25 MPa (from 5.5 to 8.75 MPa) is ignored. The level crossing method is the most appropriate for this type of loading as it gives a better correspondence between cycles and trucks. Since, as it turns out, none of the stress ranges exceed the thresholds for the details, the effect of ignoring the smaller intermediate stress ranges is inconsequential.

Each stress range over the cut-off stress of 4.5 MPa was tabulated. These stress ranges were sorted into discrete bins of 3.5 MPa intervals for each member in the floor truss. The

distributions of the stress range data for continuous periods of monitoring are presented in Tables 3-5.

Table 3: Stress Range Percentages During Constant Data Collection For the East Truss

Stress Range (MPa)	Upper Chord	Diagonal	Lower Chord
0-3.5	56.4	16.6	4.1
3.5-7	43.6	80.7	42.7
7-10.5	0.0	2.7	48.5
10.5-14	0.0	0.0	4.7

Table 4: Stress Range Percentages During Constant Data Collection For the West Truss

Stress Range (MPa)	Upper Chord	Diagonal	Lower Chord
0-3.5	65.0	49.4	9.1
3.5-7	35.0	49.8	78.4
7-10.5	0.0	0.8	11.9
10.5-14	0.0	0.0	0.6

Table 5: Stress Range Percentages During Constant Data Collection For the Floor Truss

Stress Range (MPa)	Upper Chord	Diagonal	Lower Chord
0-3.5	3.8	2.3	1.9
3.5-7	76.4	48.7	40.5
7-10.5	19.2	36.0	34.1
10.5-14	0.6	10.6	18.3
14-17.5	0.0	2.0	4.3
17.5-21	0.0	0.3	0.9
21-24.5	0.0	0.06	0.1
24.5-28	0.0	0.03	0.0

From the above tables it can be seen that the percentage of stress ranges in each bin for the east truss is very similar to that of the west truss, with slightly greater stress ranges in the east truss (under the northbound traffic). It is also notable that less than one in 1000 stress events in the diagonal of the floor truss exceeds 21 MPa and less than one in 3300 stress events in this member exceed 24.5 MPa. Not a single stress event recorded in any truss during constant data collection exceeded its fatigue threshold or CAFL for the details.

These histograms were then used to determine an effective stress range for each member using Equation 1. The fatigue damage caused by a given number of cycles of the effective stress range is the same as the damage caused by an equal number of the different stress ranges defined by the histograms. The effective stress ranges for the east, west and floor trusses are shown in Table 6. Again, the east truss seems to have slightly greater effective stress ranges.

Table 6: Effective Stress Ranges From Constant Data Collection

Member	East Truss	West Truss	Floor Truss
Upper Chord	4.04 MPa	3.78 MPa	6.89 MPa
Diagonal	5.14	4.31	13.91
Lower Chord	10.27	6.51	17.03

The gages in the east truss displayed excessive noise during triggered data collection and therefore are not included in the following discussion. The stress distributions displayed as percentages of all stress ranges recorded during triggered data collection are presented in Tables 7 and 8 and the effective stress ranges for each member of each truss are presented in Table 9.

Table 7: Stress Range Percentages During Triggered Data Collection For the West Truss

Stress Range (MPa)	Upper Chord	Diagonal	Lower Chord
0-3.5	58.5	38.6	30.0
3.5-7	41.4	61.0	43.2
7-10.5	0.0	0.4	26.4
10.5-14	0.0	0.0	0.4

Table 8: Stress Range Percentages During Triggered Data Collection For the Floor Truss

Stress Range (MPa)	Upper Chord	Diagonal	Lower Chord
0-3.5	13.3	36.8	3.0
3.5-7	51.1	30.9	24.5
7-10.5	34.2	25.5	55.0
10.5-14	1.4	5.5	14.6
14-17.5	0.0	1.0	2.7
17.5-21	0.0	0.2	0.3
21-24.5	0.0	0.04	0.01

Table 9: Effective Stress Ranges From Triggered Data Collection

Member	West Truss	Floor Truss
Upper Chord	3.83 MPa	6.6 MPa
Diagonal	4.53	7.06
Lower Chord	7.37	7.26

These distributions of triggered data are not directly comparable to the distributions shown in Tables 3-5, because a substantial number of the stress ranges are not recorded during the triggered-data periods. The triggering was based on large stress ranges in the lower chords of the trusses, therefore the distributions and effective stress ranges for the triggered data in the diagonal and upper chord of the main truss and floor truss show a larger percentage of smaller stress ranges. However, the peaks of the distributions look similar.

REVERSAL AND HIGH-TENSION-STRESS MEMBER TEST RESULTS

A limited amount of continuous open-traffic data was also taken for the reversal and high-tension-stress members of the main truss. The data were reduced in the same manner as in the open traffic tests using the algorithm programmed in Visual Basic in Excel. The individual stress events were separated into bins, and the resulting percentages of all stress events in each bin are presented in Table 10.

The effective stress range members L3U4 and U4U6 are 7.9 and 5.7 MPa, respectively. The largest stress range recorded was 22 MPa in the high-tension-stress member, L3U4. The time history of this event is presented in Figure 16. The stress ranges recorded for the reversal member, U4U6, never exceeded 13 MPa.

Table 10: Stress Range Percentages During Continuous Data Collection for the Reversal Member (U4U6) and High-Tension-Stress Members (L3U4)

Stress Range (MPa)	L3U4	U4U6
0-3.5	5.2	1.0
3.5-7	63.3	92.4
7-10.5	21.9	6.3
10.5-14	6.9	0.3
14-17.5	2.3	0.0
17.5-21	0.1	0.0
21-24.5	0.3	0.0

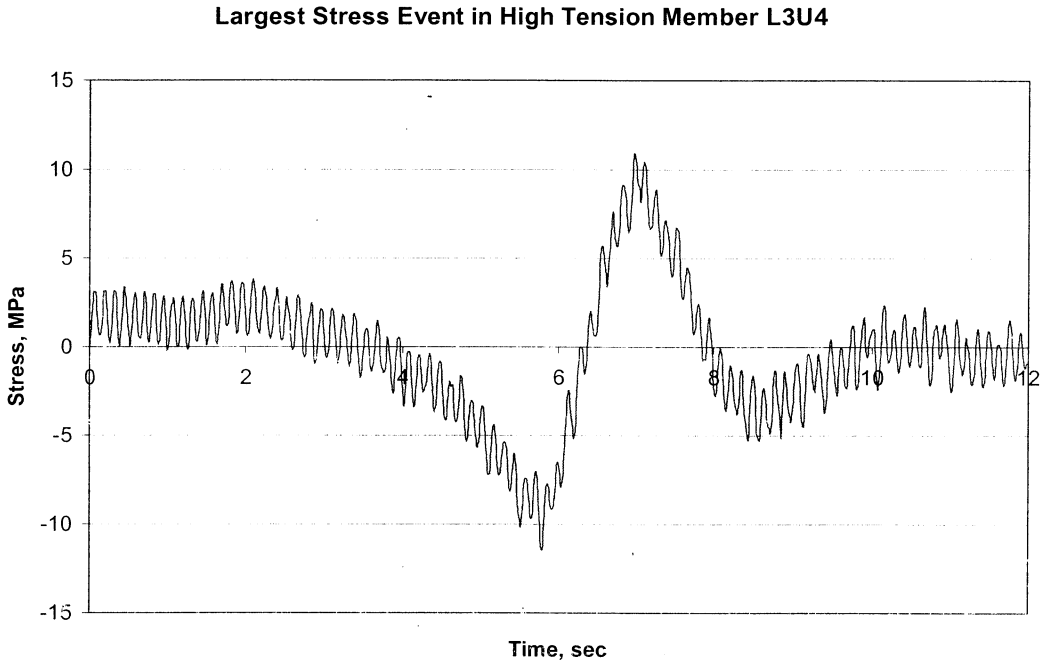

Figure 16: Largest Stress Event in High-Tension-Stress Member L3U4

CHAPTER 6

RESULTS OF ANALYSES

2-D ANALYSIS OF MAIN TRUSS

The computer program Visual Analysis was used to model the main truss and analyze the loads applied during Tests 2 and 4. First, a two-dimensional model of the main truss was created based on the plan dimensions (Figure 17). Influence lines were then calculated for the trusses across the width of the bridge and between panel points along the length of the bridge to determine how the loads would be distributed.

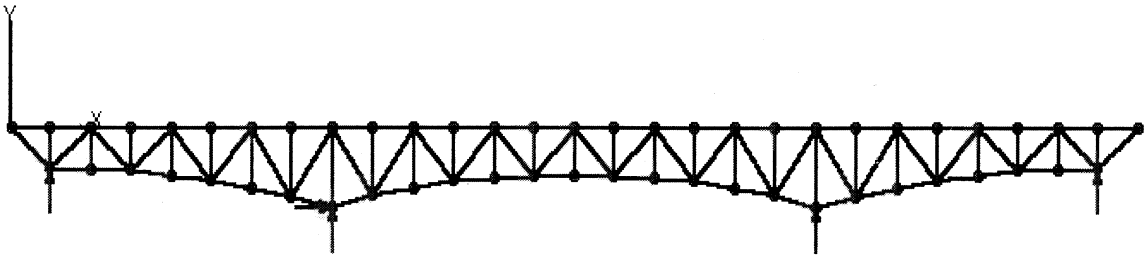

Figure 17: 2-D Visual Analysis Model of Main Truss

To apply the loads, 227 kN Mn/DOT tandem axle trucks were modeled as having only a front and rear axle spaced at 4.88 meters. We did not have measurements of each axle weight, so we assumed one third of the truck weight was placed on the front axle, and two-thirds was placed on the rear axle. This weight distribution was estimated from independent axle weigh tickets of trucks used in the study of Bridge 4654 [12].

Test 2

The load distribution across the bridge deck was first checked by plotting the time histories for an east truss and west truss member during Test 2. The percentage of the west truss member stress felt by the east truss was then compared to the percentage predicted by an influence line. The data presented in Figure 18 shows that the east truss recorded 30 percent of the stress recorded in the west truss during Test 2. Calculations from a simple influence line yield a percentage of 28, suggesting good agreement between theoretical and actual distribution.

To analyze the results of Test 2, trucks were centered in their lanes as shown in Figure 11b. By measuring the time between peaks in the stress history and estimating the trucks travel speed at 88 kph, it was determined that the following distances for the three rows of trucks was 30.5 and 39.6 meters. Loads were applied to the model with appropriate distances between them and were moved across the length of the bridge.

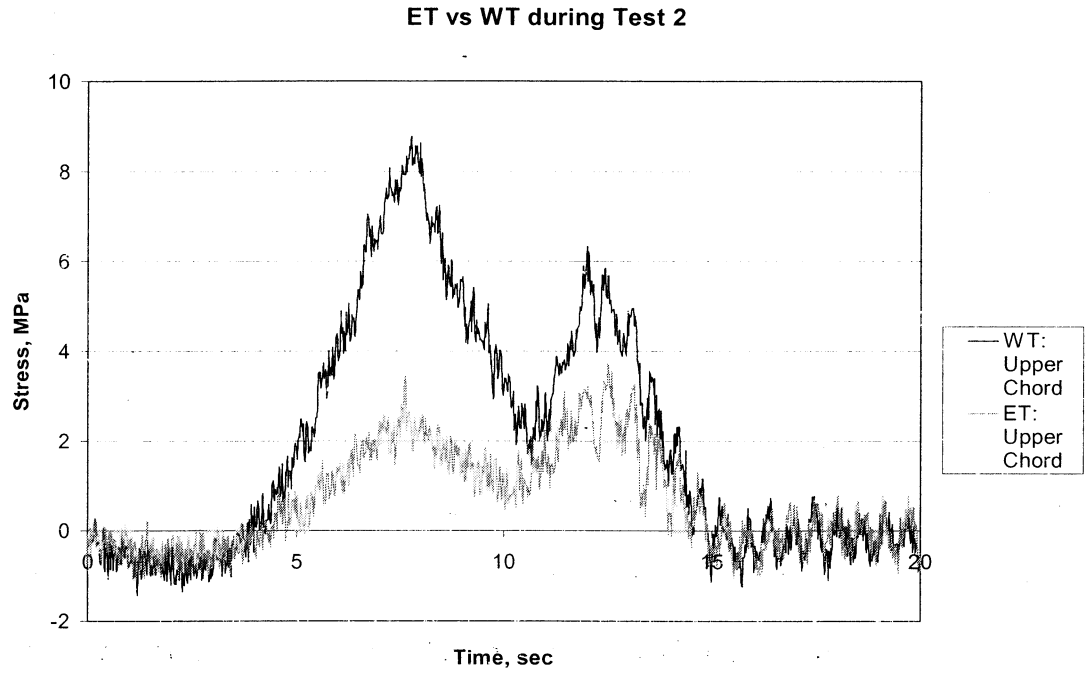

Figure 18: Distribution of Load Across the Bridge Deck

As discussed in Chapter 2, the disparity between actual and predicted stress ranges can often be attributed to unexpected partial end fixity at abutments. Therefore, the bridge was first modeled as designed with three of the four bearings defined as roller connections, allowing displacement along the length of the bridge. A second model was then made where all bearings were pin connections, restricting any longitudinal displacement. The effect of restraining the movement from the live load is to make the truss behave more like an arch, which increases the compressive force in the lower diagonal but reduces the forces in the diagonal and upper chord.

From the plots of the analytical results versus the actual time histories for Test 2 in Figure 19a-c, one can see that for the upper and lower chord, the actual stress lies somewhere in between the roller support and pinned support analyses. This is to be expected, as it is unlikely that the support neither totally restrains movement nor is completely free.

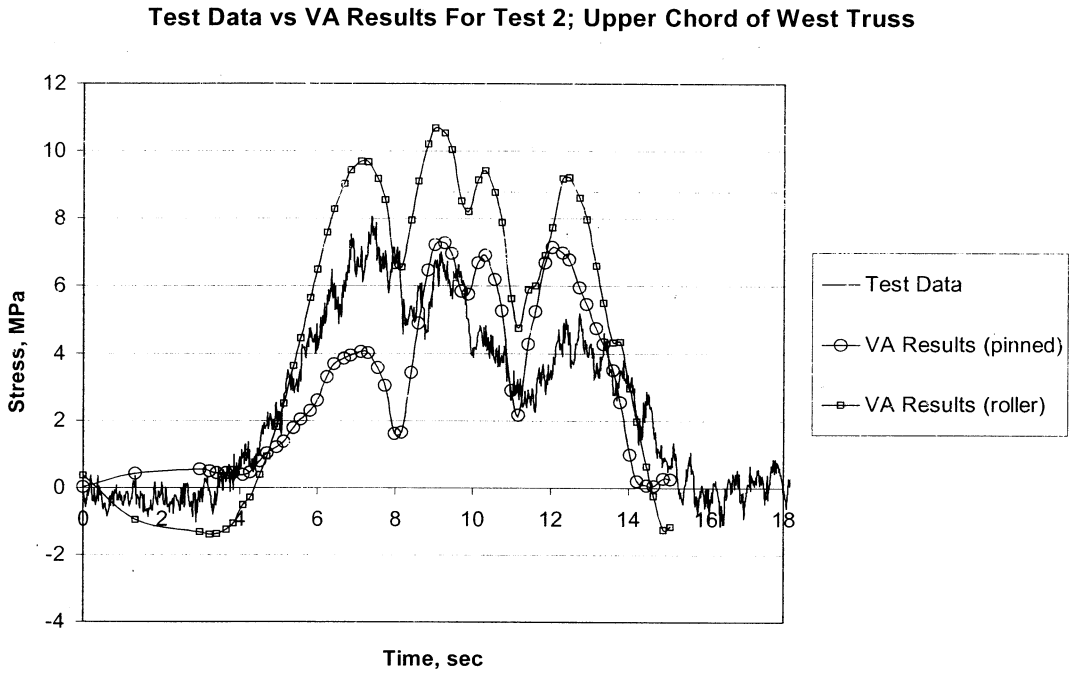

A

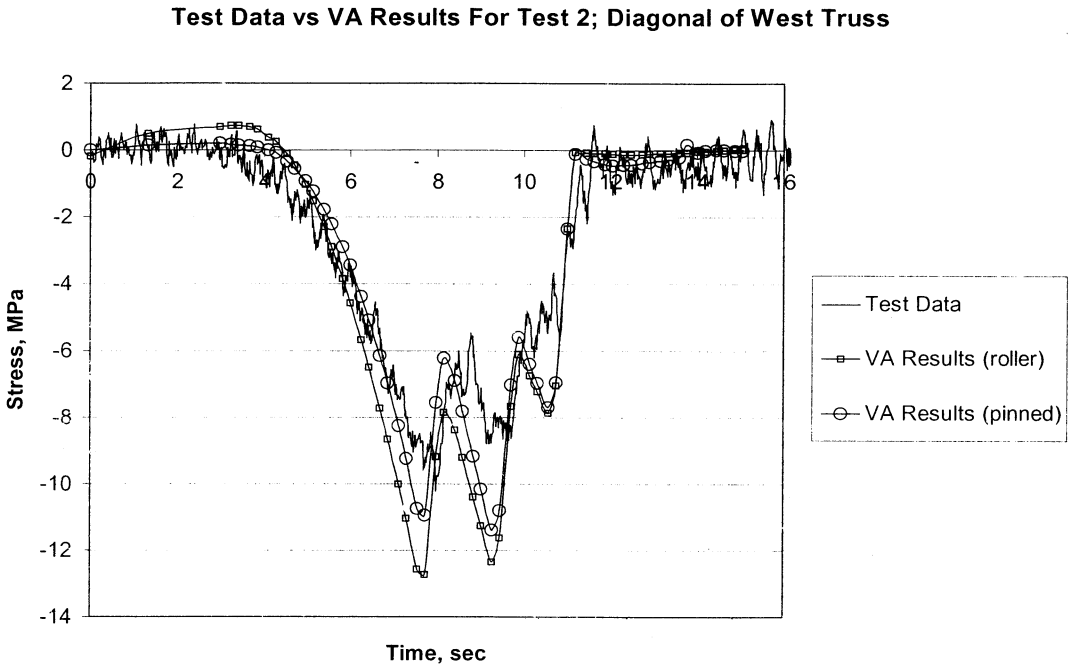

B

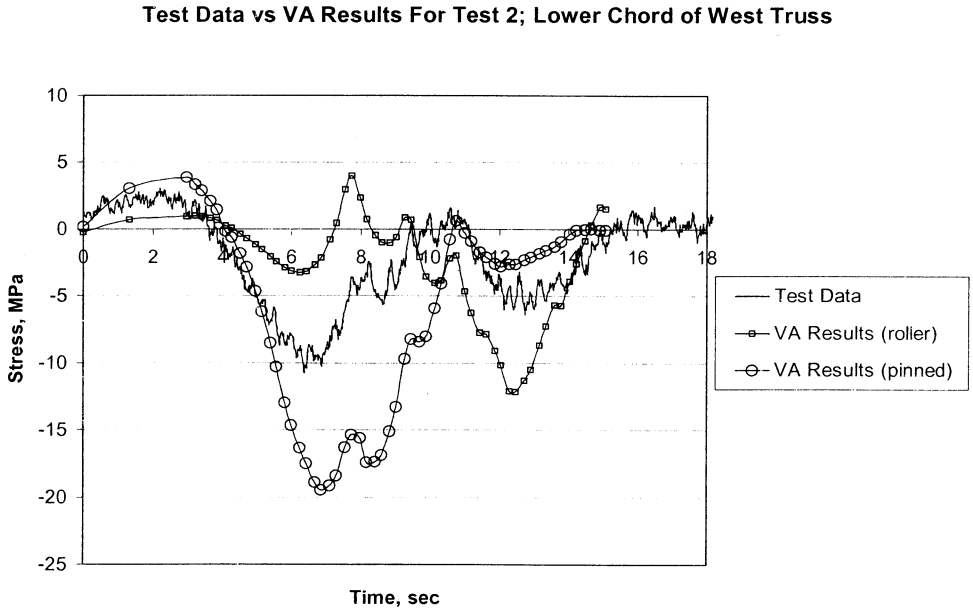

C

Figure 19: Comparison of 2-D Analysis and Test Data for Main Truss in Test 2

The resulting ratios of actual to predicted stress ranges for each member are presented in Table 11. The agreement of the upper chord and diagonal members is better with the pinned model. For the lower chord, the roller model gives a stress range that is in better agreement with the actual measured stress range. However, Figure 19c shows that the shape of the stress history is much closer to the pinned model.

Table 11: Ratio of Actual to Predicted Stresses in Main Truss for 2-D Analysis of Test 2

Member	Roller Bearings	Pinned Bearings
Upper Chord	68%	113%
Diagonal	58%	82%
Lower Chord	78%	53%

The upper chord recorded a stress range of 8 MPa during Test 2. Comparatively, analysis predicted stress ranges of 11.7 and 7.1 MPa for roller and pinned bearings, respectively. Likewise for the diagonal, the recorded stress range was 9.5 MPa and predicted stress ranges were 16.4 and 11.6 MPa for roller and pinned bearings. Lastly, for the lower chord, the recorded stress range was 12.5 MPa while the predicted stress ranges were 16.1 and 23.4 for roller and pinned bearings.

In conjunction with the unknown amount of fixity at the bearings, many other assumptions made in analysis could have led to the variance between actual and predicted stress ranges.

Test 4

Test 4 was analyzed with the same model used to analyze Test 2. The bridge pier supports were also again modeled using roller bearings and pinned bearings. Influence lines were used to determine how loads were to be applied to the model. It was assumed that the trucks were centered in each lane and aligned as shown in Figure 11d. The results of the analyses are shown in Figures 20a-c.

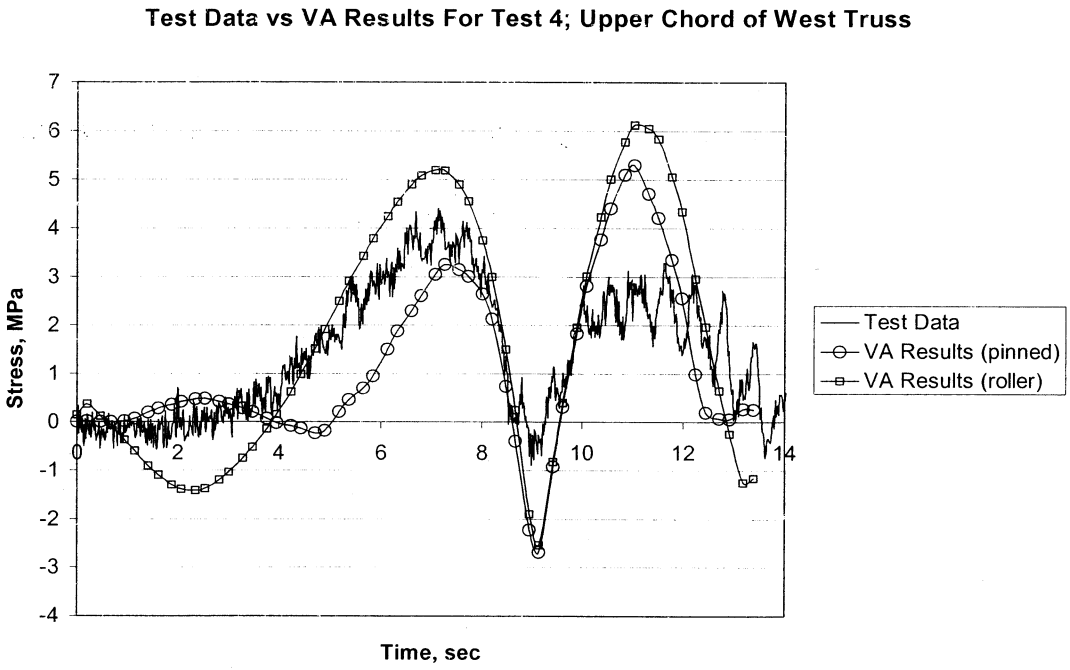

A

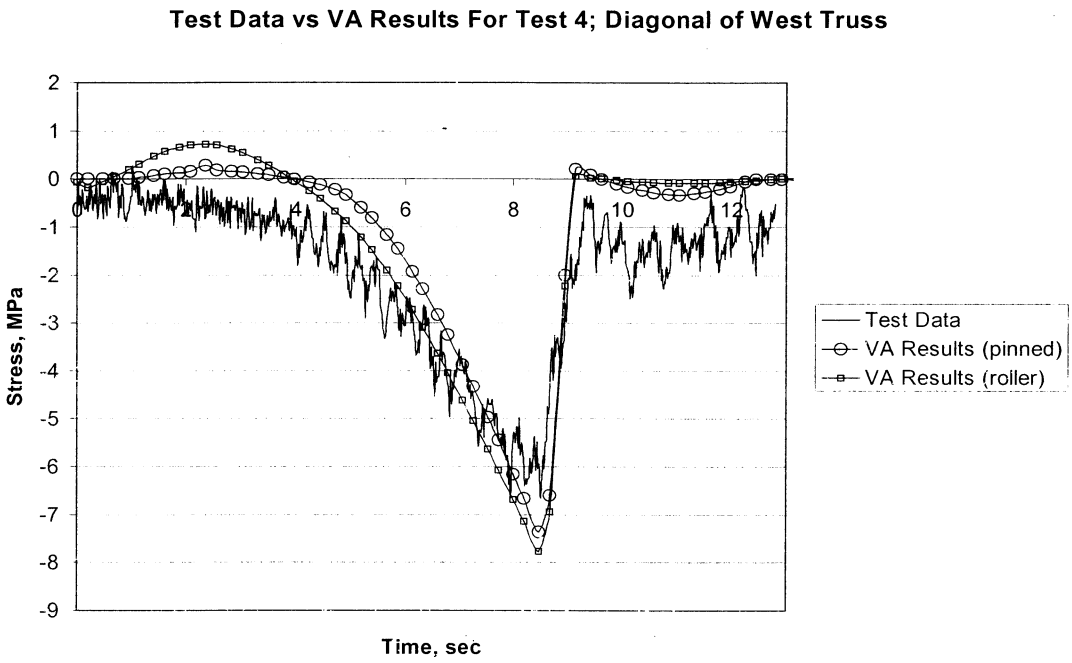

B

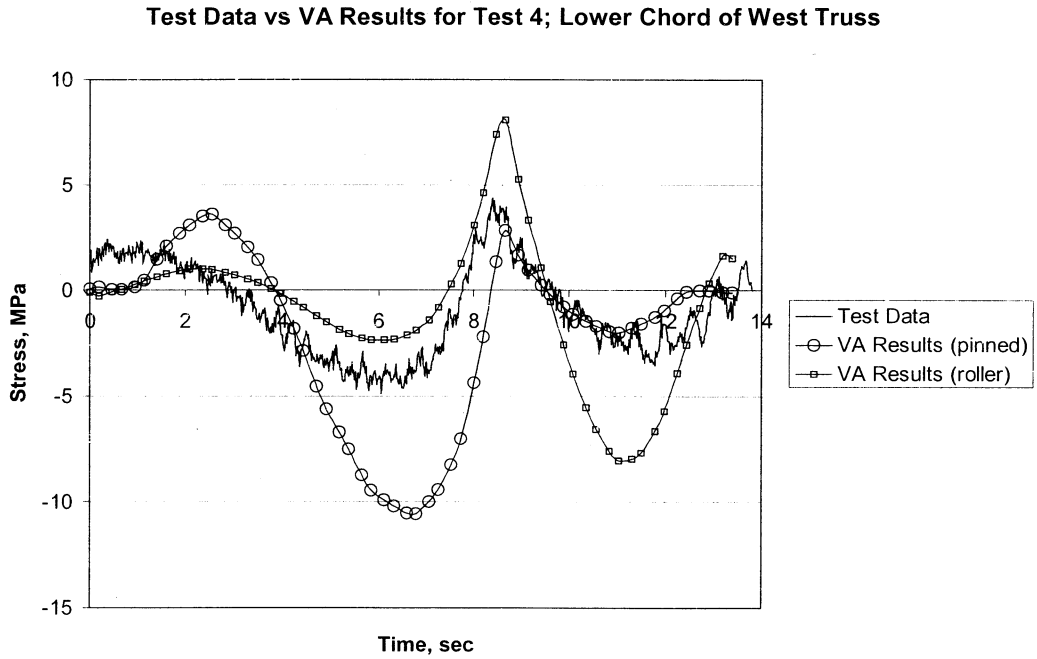

C

Figure 20: Comparison of 2-D Analysis and Test Data for Main Truss in Test 4

The results of the analyses again show that for the upper and lower chords, the actual response fall between the predictions for roller and pinned bearings. The predicted response of the diagonal also shows that the bearing type has little effect on the internal stress. This is in good agreement with the analyses for Test 2.

During Test 4 the upper chord of the main truss recorded a stress range of 5 MPa. Comparatively, analysis predicted stress ranges of 9 and 8 MPa for roller and pinned bearings, respectively. The diagonal recorded a stress range of 6 MPa and predicted stress ranges were 9 and 8 MPa for roller and pinned bearings. Finally, the lower chord recorded a stress range of 8 MPa while the predicted stress ranges were 16 and 14 for roller and pinned bearings. The resulting ratios of actual to predicted stress ranges for each member are presented in Table 12.

Table 12: Ratio of Actual to Predicted Stresses in Main Truss for 2-D Analysis of Test 4

Member	Roller Bearings	Pinned Bearings
Upper Chord	58%	63%
Diagonal	71%	78%
Lower Chord	50%	56%

The ratios of actual to predicted stresses are much more consistent for Test 4 than for Test 2. This is most likely due to the fact that the formation for Test 4 was easier to maintain than the Test 2 formation. Here the analyses with pinned bearings were consistently more accurate than that with roller bearings.

3-D ANALYSIS OF TRUSS SYSTEM

As discussed in Chapter 2, unexpected composite action between the deck and stringers in bridges often occurs, resulting in different values for actual and predicted stresses. To try and refine the analyses conducted on the main truss, a three-dimensional model incorporating the concrete deck was constructed using SAP2000. For simplicity, the deck was modeled as a beam running transverse to the roadway with a thickness of 16.5 cm (the actual thickness of the deck) and a width of 8.0 m, the effective width given the span length as defined by ACI [23]. Instead of sitting atop stringers, short, stiff stub columns were used. W27x539 shapes were selected for the columns for maximum stiffness and placed at the nodes of the upper chords of the floor truss .(Figure 21).

Since the 3-D analysis is meant to refine the current analyses, it was only applied to Test 4 as it was the most accurate and consistent under 2-D analysis. The bearings were again modeled as both roller and pinned supports. The results of the analyses are presented in Figure 22a-c.

The stress ranges were more accurate for the upper chord and diagonal, but the stress ranges in the lower chord ranged from worse when the bearings were modeled as rollers to only slightly better with pinned bearings. In the upper chord, the predicted stresses for roller and pinned bearings were 5.2 and 5.4 MPa, respectively, compared to an actual stress range of 5 MPa. The diagonal recorded a stress range of 6 MPa while the analyses predicted 11.4 and 11.7 MPa for the roller and pinned bearings. Lastly, the lower chord recorded a stress range of 8 MPa and analyses predicted 16 and 11.7 MPa for the roller and pinned bearings. The ratio of actual to predicted stress ranges is presented in Table 13.

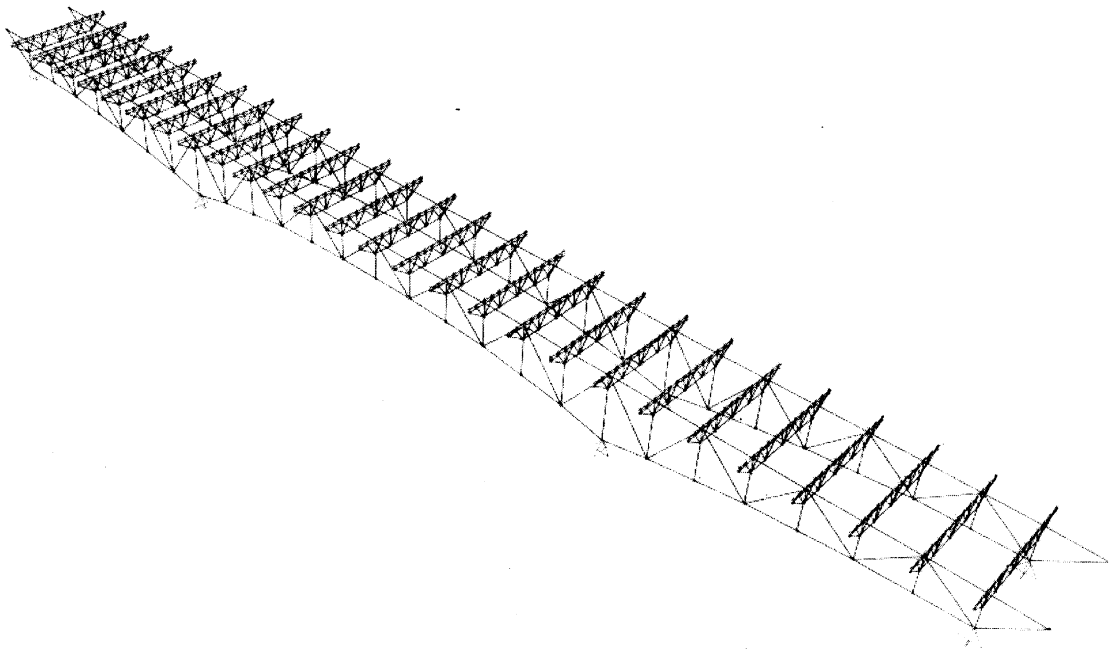

Figure 21: 3-D SAP2000 Model

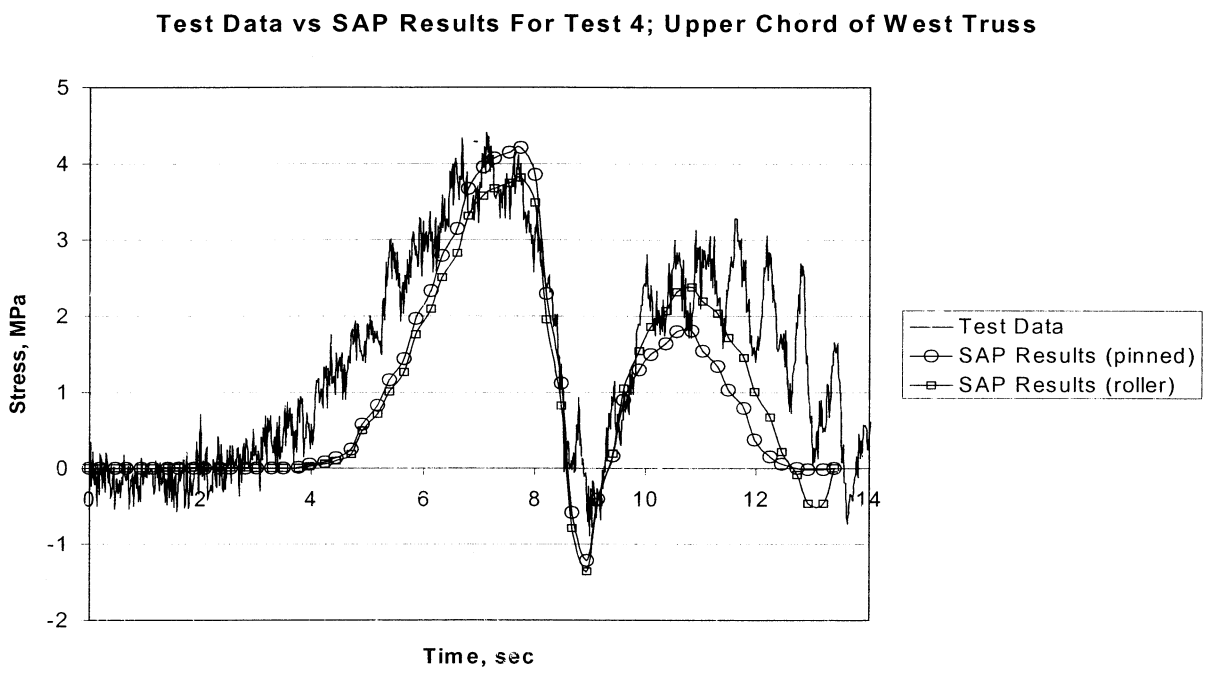
Test Data vs SAP Results For Test 4; Upper Chord of West Truss
Stress, MPa
Time, sec
Test Data
SAP Results (pinned)
SAP Results (roller)

A

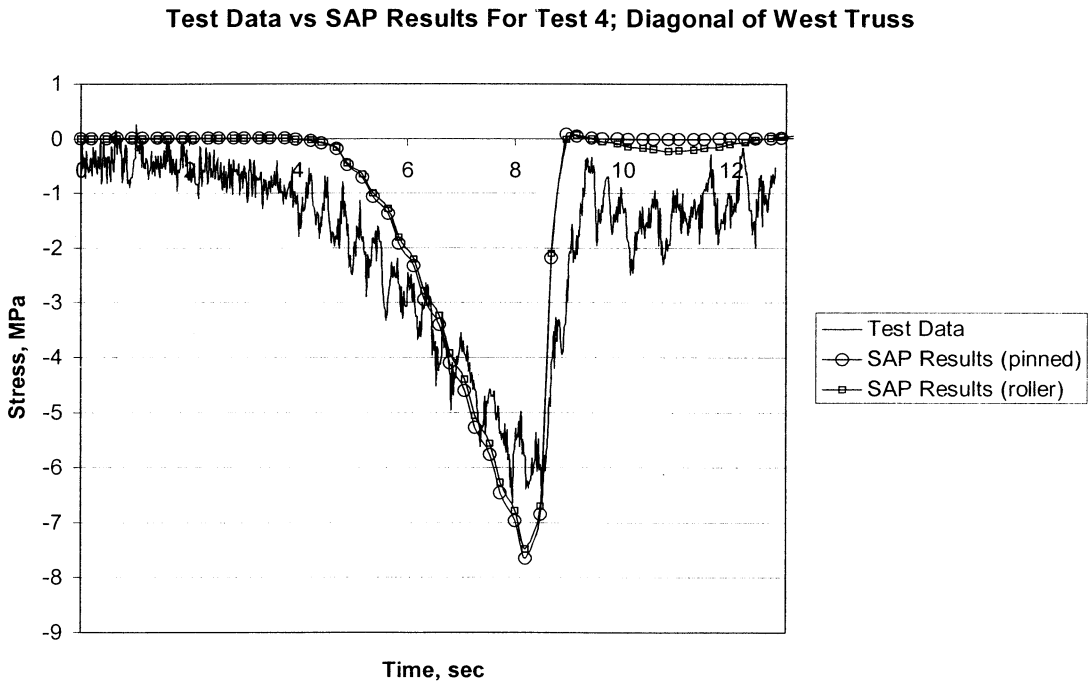
Test Data vs SAP Results For Test 4; Diagonal of West Truss
Stress, MPa
Time, sec
Test Data
SAP Results (pinned)
SAP Results (roller)

B

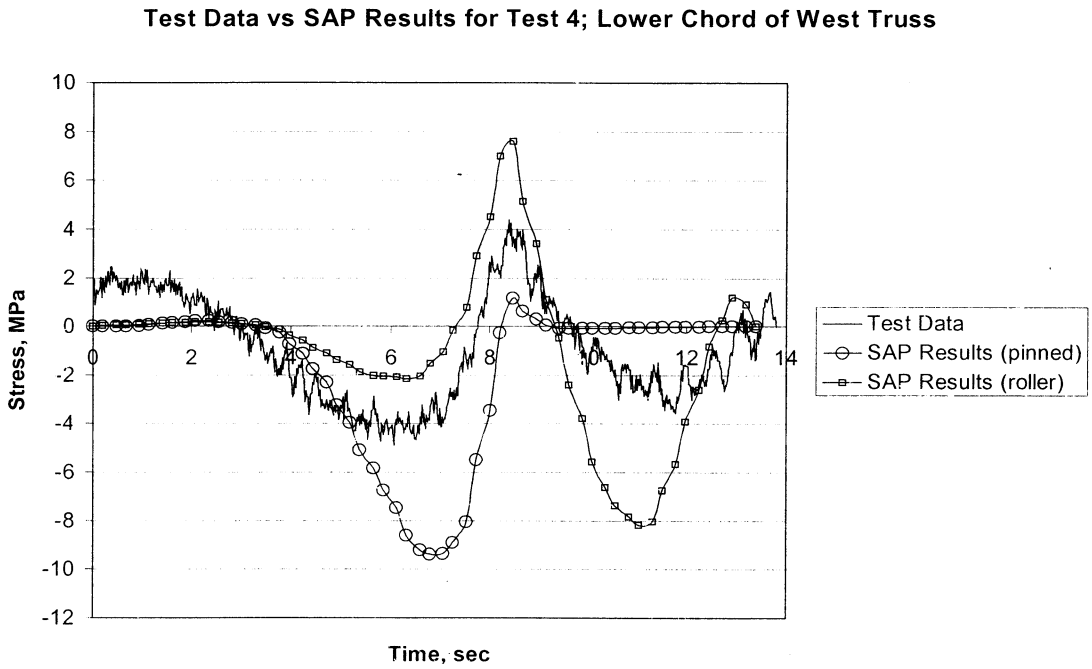

C

Figure 22: Comparison of 3-D Analysis and Test Data for Main Truss in Test 4

Table 13: Ratio of Actual to Predicted Stresses in Main Truss for 3-D Analysis of Test 4

Member	Roller Bearings	Pinned Bearings
Upper Chord	96%	93%
Diagonal	80%	78%
Lower Chord	50%	75%

The type of bearing used in analysis had minor effects on the results for the upper chord and diagonal, however, the predicted response of the lower chord changed drastically. The total stress range of the lower chord was 75 percent of the actual stress range using pinned bearings in the model, however, once the row of trucks passed over the pier to the south of the lower chord, the predicted stresses went to zero. When the bearing to the south of the lower chord is pinned, it prevents any horizontal load from being transferred to the lower chord. The fact that the lower chord did feel load after the trucks passed the bearing to the south of it again confirms the assumption that the bearings are neither fully restrained nor free to displace.

The ratio of actual to predicted stresses in the diagonal were the same as in the 2-D analysis when pinned bearings were used, however, the ratio increased by nine percent from the 2-D analysis when roller bearings were used. Still, the predicted response for the diagonal changed the least under 3-D analysis. This follows that there are not any alternative load paths for the flow of shear force in the truss regardless of changes made at the upper or lower chords.

The upper chord predictions changed the most from the 2-D to 3-D analysis. By adding the concrete deck, the effective depth of the truss was slightly increased thus lowering the predicted stresses in the upper chord. This confirms that the concrete deck contributes a significant amount of stiffness to the truss system and should be included in any model of the bridge.

POSSIBLE PROBLEM MEMBERS AND REMAINING LIFE IN MAIN TRUSS

Based on the completed analysis and recorded stress ranges in open traffic conditions, members that may exceed the fatigue limit can be identified. The largest stresses recorded in testing occurred during Test 2. The results from a Visual Analysis model using this loading and both pinned and roller bearings are shown in Table 14.

Table 14: Predicted Stresses Exceeding Fatigue Limit During Test 2

Member	Roller Bearings	Pinned Bearings
U2L3	54 MPa	42 MPa
L3U4	49	47
U4U6	56	40

When the roller bearings are assumed, the analysis predicts that members U2L3, L3U4, and U4U6 could experience stress ranges slightly larger than the 48 MPa CAFL for the Category D details (the short clips on the diaphragms). However, when the bearings are assumed pinned, which was shown to be the more accurate assumption, the predicted stress ranges do not exceed the CAFL. Even with the pinned assumption, however, the analysis still over-predicts the stress ranges significantly. Therefore the actual stress ranges due to this loading would be even less than the stress ranges in Table 14.

The first two of these members are diagonals while the last is an upper chord. The ratio of actual to predicted stresses for diagonals and upper chords was consistently between 58 and 78 percent for the 2-D analysis of Test 4. If the largest ratio were applied to the predicted stress ranges in Table 14, the resulting stress ranges would all fall well below the CAFL (Table 15). Therefore,

all stress ranges for all members in the main truss fall below the fatigue limit for a Category D detail and remaining life for this structure is infinite.

Table 15: Corrected Predicted Stresses For Problem Members During Test 2

Member	Roller Bearings	Pinned Bearings
U2L3	42.1 MPa	32.8 MPa
L3U4	38.2	36.7
U4U6	43.7	31.2

2-D ANALYSIS OF FLOOR TRUSS

Visual Analysis was also used to create a two-dimensional model of the floor truss to analyze Tests 1 and 4 (Figure 23). A concrete deck was incorporated into the model to account for added strength from unexpected composite action. As in the 3-D analysis, the deck was modeled as a 16.5 cm by .8 m beam resting atop stiff stub W27x539 columns.

Test 1

To get analytical results for the first test, the front axle of a truck was assumed to be 4.57 meters away from the rear axle of the truck directly in front of it. An influence line for the floor truss showed that the load on the truss would be largest when the rear axle of the center truck was directly on the truss. For simplicity, a single load for each axle was applied at the center of each interior lane. The maximum stress range during this test occurred in the lower chord and measured 28 MPa. The analysis yielded a maximum stress for the same member of 36.7 MPa, yielding an actual to predicted stress range ratio of 76 percent. If the distance between the front and rear axles was reduced to 3.05 meters, the analysis yielded a maximum stress in the lower chord of 42.8 MPa, a ratio of 65 percent.

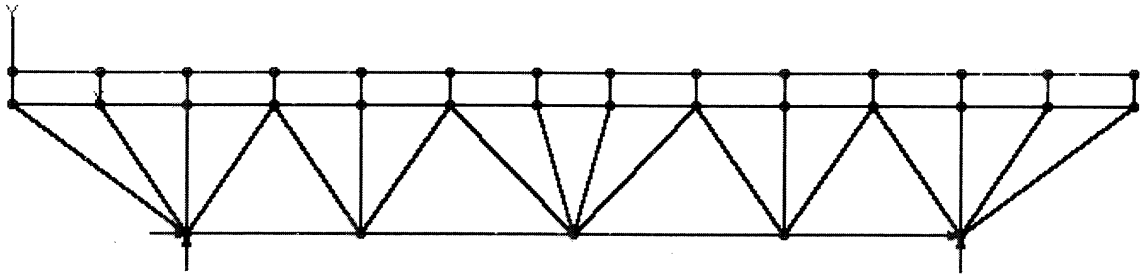

Figure 23: 2-D Visual Analysis Model of Floor Truss with Concrete Deck

Test 4

Analyses of the floor truss results for the fourth test were done in much the same way. Truck loads were applied to an influence line, which was used to determine the load distribution between neighboring floor trusses as the line of trucks moved across the bridge. Analysis was done with and without the concrete deck in place. Later, these results were averages. The time histories for each member of the floor truss versus the analysis results are shown in Figures 24a-c.

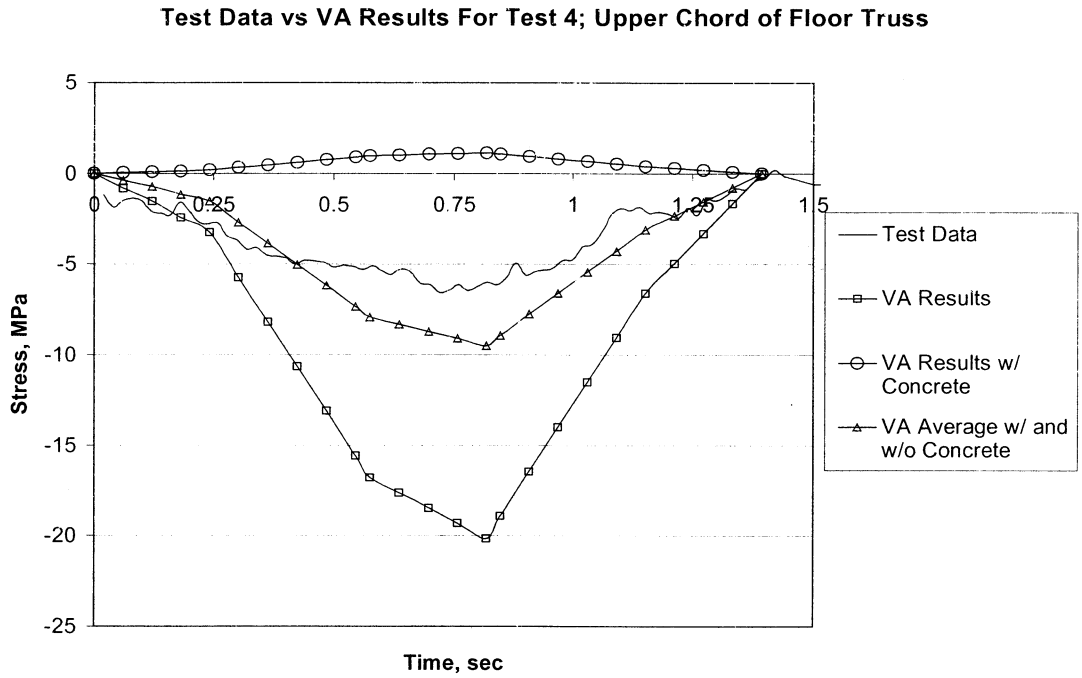

A

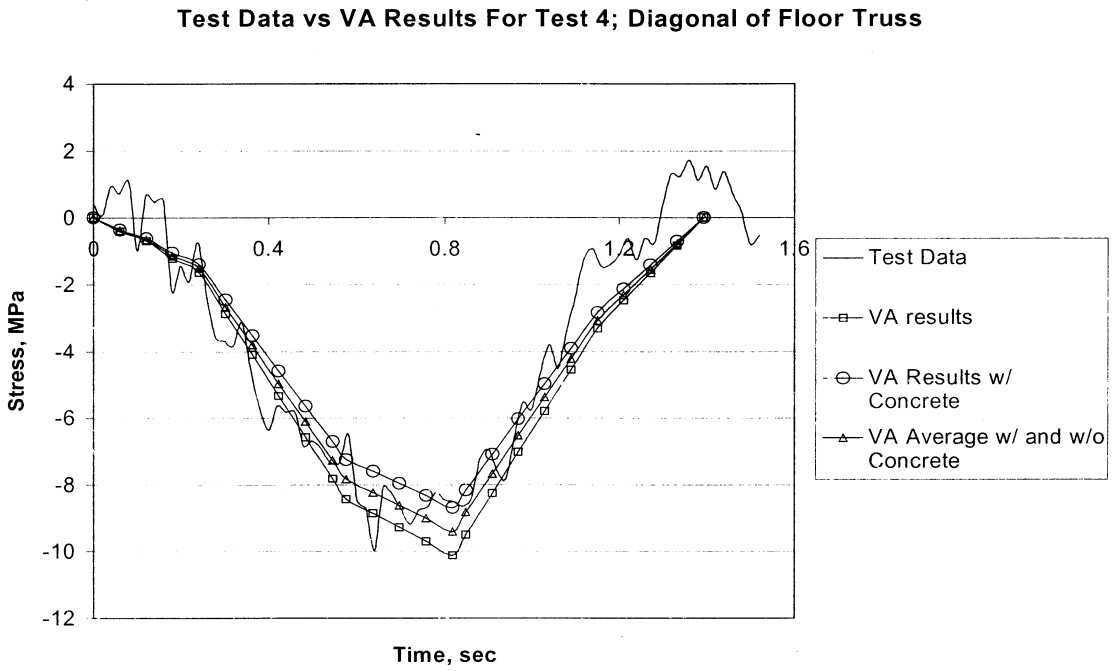

B

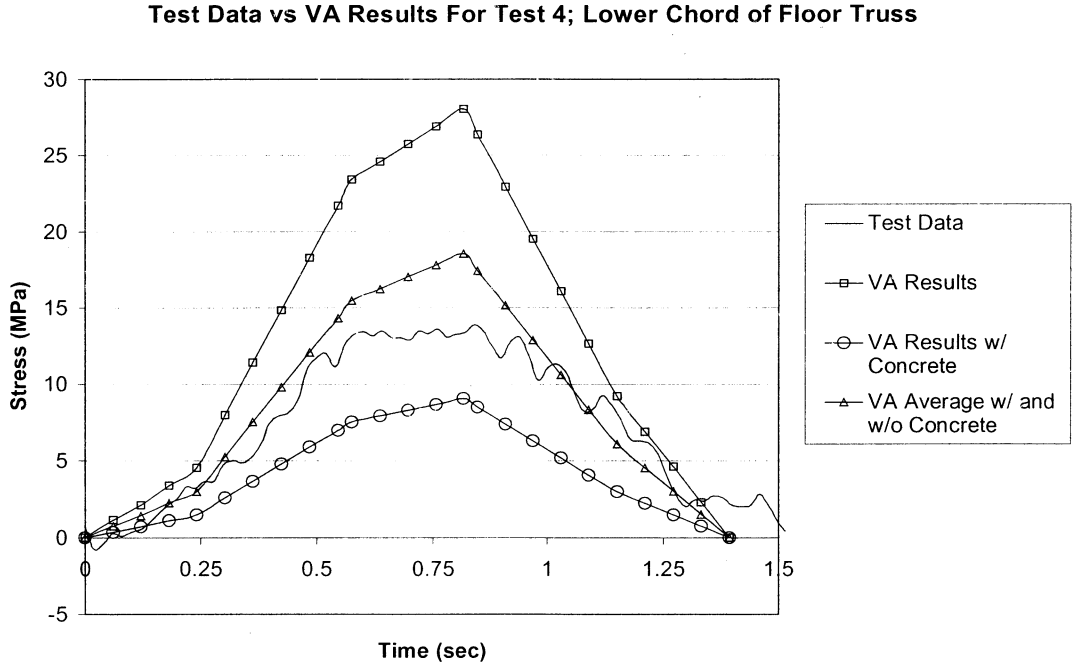

C

Figure 24: Comparison of 2-D Analysis and Test Data for Floor Truss in Test 4

From these figures, it can be seen that the analysis results from the upper chord and lower chord without the concrete deck in place are much higher than the recorded stresses. Including the deck lowers the stresses too much so the two separate predicted responses were averaged to estimate the contribution of the concrete deck. This averaged predicted response shows the best correlation to the actual response. The ratio of actual to predicted stress ranges is shown in Table 16.

Table 16: Ratio of Actual to Predicted Stresses in Floor Truss for 2-D Analysis of Test 4

Member	VA Results	VA w/ Concrete	Average
Upper Chord	33%	n/a	69.5%
Diagonal	91%	106%	98%
Lower Chord	49.5%	154.4	74.7%

The stress ranges felt in the diagonal are only slightly affected by the concrete deck. This follows the results of diagonals in the other analyses. There are no alternative load paths at the diagonals, therefore a change in supports or the addition of a concrete deck have little effect.

REMAINING LIFE OF THE FLOOR TRUSS

The predicted stress ranges in the floor truss never exceed the CAFL of 31 MPa for the Category E (stiffener) detail, therefore the remaining life of the floor truss is considered to be infinite. The largest predicted stress range for Test 4 occurs in member L1U4 and is 22.2 MPa when the results of the models with and without the concrete deck are averaged. Since this member is a diagonal, one can assume that the actual stress range in the member correlated well with the predicted stress range.

CHAPTER 7

SUMMARY AND CONCLUSIONS

Field tests and analyses were conducted on Bridge 9340 crossing the Mississippi River just east of downtown Minneapolis. Field tests were conducted in two parts. The first part involved measuring strains while trucks of known weights crossed the bridge. The second part involved monitoring the strains and counting strain cycles under open traffic conditions over a period of several months. Results of the first part were used to calibrate two and three-dimensional numerical models. Results of the second part were used to characterize the statistical distribution of the stress ranges and estimate the remaining fatigue life. The main conclusions were:

1. Inspection of the bridge revealed Category D details on the main truss members and Category E members on the floor truss. No fatigue cracks were found by visual inspection of those members.

2. The largest stress range measured in the main truss during the controlled tests was 12.5 MPa in the lower chord, from three rows of three trucks. The analyses show that member U4U6 would have the largest stress range from this loading, 46 MPa. This is less than the fatigue threshold for the most critical details on these members, which is 48 MPa for Category D.

3. The largest stress range in the main truss during the open-traffic monitoring was 22 MPa and this was in another member, L3U4.

4. The agreement of the analyses with the measured stress ranges was best when a three-dimensional model of the whole bridge was analyzed. In both the two-dimensional and three-dimensional analyses, the agreement was best if the roller bearings at the piers were assumed to be pinned so that a horizontal reaction developed and arching action occurred.

5. The largest stress range measured in the floor truss during the controlled tests was 28 MPa in the lower chord, from three rows of trucks in the leftmost lane (closest to the center) in each direction. This is less than the fatigue threshold of 31 MPa for a Category E detail.

6. The largest stress range in the floor truss during the open-traffic monitoring was 25 MPa and this was in a diagonal.

7. Two-dimensional analyses were adequate for the floor truss. Very poor agreement with the measured results was obtained unless some composite action with the deck was assumed. Full composite action was too much, and optimal results were obtained by averaging the results from the non-composite case and the fully composite case.

8. Since the measured and calculated stress ranges were less than the fatigue threshold, it is concluded that fatigue cracking is not expected in the deck truss of this bridge.

9. Live-load stress ranges greater than the fatigue threshold can be calculated if the AASHTO lane loads are assumed. The actual measured stress ranges are far less primarily because the loading does not frequently approach this magnitude. While the lane loads are appropriate for a strength limit state (the loading could approach this magnitude a few times during the life of the bridge), only loads that occur more frequently than 0.01% of occurrences are relevant for fatigue. For this bridge with 15,000 trucks per day in each direction, only loads that occur on a daily basis are important for fatigue.

The following actions are recommended:

1. The members of the main truss with the highest stress ranges are U2L3, L3U4 and U4U6. These members should be inspected thoroughly, especially at the ends of the "clips" on the diaphragms in the tension members and at any intermittent fillet welds. These members should be inspected every two years as is presently done.

2. The lower chords and diagonals of all the floor trusses also have high stress ranges. The ends of the "fin" attachments reinforcing the splice welds are the most critical locations. Since these can be inspected easily from the catwalk, they could be inspected every 6 months.

CHAPTER 8

REFERENCES

1. Standard Specifications for Highway Bridges, American Association of State Highway Officials, Washington DC, 1961.

2. Fisher, J.W., Frank, K.H., Hirt, M.A., and McNamee, B.M., "Effect of Weldments on the Fatigue Strength of Steel Beams", National Cooperative Highway Research Program Report 102, Highway Research Board, Washington, D.C., 1970.

3. Fisher, J.W., Albrecht, P.A., Yen, B.T., Klingerman D.J., and McNamee B.M., "Fatigue Strength of Steel Beams With Welded Stiffeners and Attachments," National Cooperative Highway Research Program Report 147, Transportation Research Board, Washington, D.C., 1974.

4. Fisher, J.W., Nussbaumer, A., Keating, P.B., and Yen, B.T., "Resistance of Welded Details under Variable Amplitude Long-Life Fatigue Loading", National Cooperative Highway Research Program Report 354, Transportation Research Board, Washington, D.C., 1993.

5. Guide Specifications for Fatigue Design of Steel Bridges, American Association of State Highway and Transportation Officials, 1st Ed., Washington, D.C., 1989.

6. Standard Specifications for Highway Bridges-LRFD, American Association of State Highway and Transportation Officials, 1st Ed. Washington DC, 1994.

7. Hall, D.H., Heins, C.P., Hyma, W.R., Kostem, C.N., Krisnamurthy, N., Lally, A, Loveall, C.L, Smith, E.A., Sweeny, R.A.P, Tartaglione, L.C., and Yoo, C.H., "State-of-the-Art Report on Redundant Bridge Systems", Journal of Structural Engineering, Vol. 111, No. 12, December, 1985.

8. Ressler, S.J., and Daniels, J.H, "Fatigue Reliability and Redundancy in Two-Girder Steel Highway Bridges", Advanced Technology for Large Structural Systems Report No. 92-01, January 1992.

9. Faber, M.H., Val, D.V., and Stewart, M.G., "Proof Load Testing for Bridge Assessment and Upgrading", Engineering Structures, Vol. 22, pp 1677-1689, 2000.

10. Moses, F., Schilling, C.G., and Raju, K.S., "Fatigue Evaluation Procedures for Steel Bridges," National Cooperative Highway Research Program Report 299, Transportation Research Board, Washington DC, 1987.

11. Zwerneman, F.J., Poynter, P.G., Abbas, M.D., Rauf, A. and Yang, J., "Fatigue Assessment of Bridge Members Based on In-Service Stresses", Oklahoma State University, 1996.
12. Dexter, R.J., Hajjar, J.F., O'Connell, H.M., Bergson, P.M., "Fatigue Evaluation of Stillwater Bridge (Bridge 4654)," Minnesota Department of Transportation, 1998.

13. Dexter, R.J., Fisher, J.W., "The Effect of Unanticipated Structural Behavior on the Fatigue Reliability of Existing Bridge Structures", Structural Reliability in Bridge Engineering, Frangopol, D. M. and Hearn G. eds., Proceedings of a Workshop, University of Colorado at Boulder, 2-4 October 1996, McGraw-Hill, New York, pp. 90-100, 1996.

14. Burdette, E.G. and Goodpasture, D.W., "Correlation of Bridge Load Capacity Estimates With Test Data" National Cooperative Highway Research Program Report 306, Transportation Research Board, Washington, D.C., 1988.

15. Bakht, Baidar and Jaeger, L.G., "Bridge Testing-A Surprise Every Time", Journal of Structural Engineering, Vol. 116, No. 5, May 1990.

16. Bakht, Baidar, "Ultimate Load Test on a Slab-on-Girder Bridge", Structural Res. Rep., SRR-88-03, Ministry of Transportation, Downsview, Ontario, Canada, 1988.

17. Hahin, C., South, J.M., Mohammadi, J., and Polepeddi, R., "Accurate and Rapid Determination of Fatigue Damage in Steel Bridges", Journal of Structural Engineering, Vol. 119, No. 1, January 1993.

18. Miner, M.A., "Cumulative Damage in Fatigue", Journal of Applied Mechanics, 12, A-159, 1945.

19. Dexter, R.J. and Fisher J.W., "Fatigue and Fracture", Handbook of Structural Engineering, Chapter 24, Chen, W. F. ed., CRC Press LLC, New York, 1997, pp 24-1 to 24-30.

20. Dexter, R.J. and Fisher, J.W. "Fatigue and Fracture", Handbook of Bridge Engineering, Chapter 53, Chen, W. F. ed., CRC Press LLC, New York, 1999, 24 pages.

21. Wilson, Pete, "In-Depth Fracture Critical Bridge Inspection Report Bridge #9340: I35W over the Mississippi River (Downtown Minneapolis)," Minnesota Department of Transportation, 1997.

22. Bergson, Paul, Letter to Minnesota Department of Transportation, 21 December, 1998.

23. Code Requirements for Structural Concrete, American Concrete Institute, 1995.